

Air-LUSI: Estimation, Filtering, and PID Tracking Simulation

Andrew Cataford
Mechanical Engineering
University of Guelph
Guelph, Ontario, Canada
acatafor@uoguelph.ca

S. Andrew Gadsden
Mechanical Engineering
University of Guelph
Guelph, Ontario, Canada
gadsden@uoguelph.ca

Kevin Turpie
Sciences and Exploration
Directoriate, NASA
Greenbelt, Maryland
kevin.r.turpie@nasa.gov

Mohammad Biglarbegian
Mechanical Engineering
University of Guelph
Guelph, Ontario, Canada
mbiglarb@uoguelph.ca

Abstract—This paper describes the development of a two degree of freedom (2DoF) pointing and tracking simulation used for evaluating the Air-LUSI subsystem behaviour. The Air-LUSI project intends on obtaining high altitude Lunar Spectral Irradiance (LUSI) measurements of the Moon by integrating an automated telescope mount capable of acquiring the Moon as a target and tracking it from the science pod of an ER-2 aircraft as it flies at an altitude of 65,000 feet. By obtaining precise measurements of the Lunar Spectral Irradiance, a Lunar Calibration Model can be used for NASA's Earth Observing System (EOS). The simulations found within this report describe the estimation, filtering, and control strategies applied to the 2DoF gimbal design and compares the tracking accuracy when using system measurements or state estimates produced by the linear Kalman filter (KF) or the nonlinear unscented Kalman filter (UKF) as the input to the PID controller. An additional aspect of this project studies the nonlinear or linear system behaviour described by the interacting multiple model (IMM) algorithm and analyzes the results of a hybrid adaptive control strategy that combines the KF and UKF PID gains using the IMM mode probabilities.

Index Terms—estimation, filtering, PID control, tracking

I. INTRODUCTION

The Lunar Spectral Irradiance project (LUSI) is a NASA sponsored interagency collaboration that combines the experience and expertise of professionals at the National Institute of Standards and Technology (NIST), Hawk Institute for Space Sciences, University of Maryland Baltimore County (UMBC), and the University of Guelph. The project is one part of NASA's initiative to develop a Lunar Model for calibrating their Earth Observing System (EOS). The EOS is a series of satellites that are responsible for monitoring the geological, meteorological, oceanographic and atmospheric conditions of our planet. Existing inaccuracies within the current EOS calibration methods are preventing the system from monitoring the small climatic changes that occur within short durations of time. By obtaining a highly accurate Lunar Calibration model, the EOS should be able to detect atmospheric, climatic, and oceanographic changes with a much higher resolution.

Phase one of LUSI, was responsible for measuring the spectral irradiance of the moon using an Earth based system in Flagstaff, Arizona. Although the previous measurement system operated as intended, there was still significant radiometric uncertainty produced by the Earth's atmosphere. The reduced

accuracy of Earth based measurements pose additional challenges when vicariously calibrating the EOS equipment. By obtaining highly accurate radiometric measurements of the moon at high altitudes, the uncertainties associated with the Lunar Calibration model can be reduced and allow for high resolution monitoring of our planets changing climate.

Phase two of the LUSI project, renamed Air-LUSI, intends on integrating a retrofitted version of the LUSI design into the science pod of NASA's ER-2 aircraft; establishing a mobile lunar observatory and the second airborne telescope in NASA's fleet of aircrafts. The ER-2 aircraft will fly at an altitude of 65,000 feet, and allow for accurate measurements of the Lunar reflectance that has otherwise been unachievable from ground based equipment or orbiting systems.

A. Subsystem Description:

To achieve pointing within the Elevation and Azimuth coordinates, the subsystem design requires 2DoF. In this particular design, the freedom of motion is obtained using two bisecting axes that produce a 2DoF gimbal. The subsystem design uses two linear actuators to control the pointing of the telescope. One linear actuator is used to control the elevation angle of the telescope within the YZ plane, and the other actuator controls the incline angle of the telescope with respect to the YZ plane as shown by the blue and red lines in Figure 1.

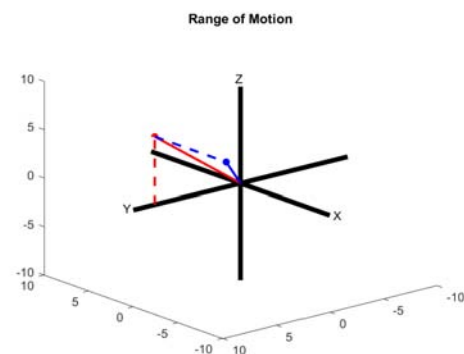


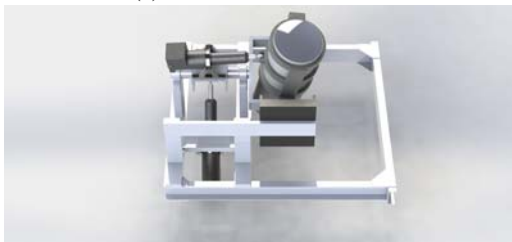
Fig. 1: 2DoF Motion

Although our design does not operate with the conventional Elevation and Azimuth coordinate system used in most ce-

restrial observations, the Elevation and Incline angles of the subsystem can still achieve the same pointing coordinates. All range of motion within the 2DoF is limited by the position of the linear actuators with respect to their axis of rotation, and their associated stroke lengths. The renderings found in Figure 2 show the design concept of the subsystem along with the range of motion described by Figure 1.



(a) Elevation in YZ Plane



(b) Telescope inclination relative to YZ plane

Fig. 2: Subsystem Design

B. Simulation Objective:

The purpose of the simulations described within this report are to determine the possible benefits of using the state estimates produced by KF, UKF, and IMM to obtain the error signals used by the PID controllers. The primary theory is that significant benefits in terms of control, stability, and accuracy can be obtained when using the error signals produced by the filters compared to the noisy measurements obtained from the system directly.

To quantitatively assess the improved tracking ability when using the filtered state estimates as the input to the PID controller, we must simulate the system's ability to track the Moon as it moves along a specified trajectory for the four cases listed below. The following list provides a summary of the simulation objectives that are addressed in subsequent sections.

Objective Summary:

- 1) Simulate Unfiltered Non Linear Model using noisy measurements for PID Error Signal
- 2) Simulate Linear KF model using state estimates for PID Error Signal
- 3) Simulate Non Linear UKF model using state estimates for PID Error Signal
- 4) Simulate IMM estimates for PID Error Signal and mode probability for adaptive control

The second purpose of the simulation is to determine whether the linear KF model can accurately estimate the states

of the non linear system and whether the true system behaviour can be characterized by two different modes of operation. If the system exhibits different behaviours, the IMM can possibly yield an adaptive control strategy by modifying the PID gains with respect to the two different mode probabilities as shown in Figure 3 [?].

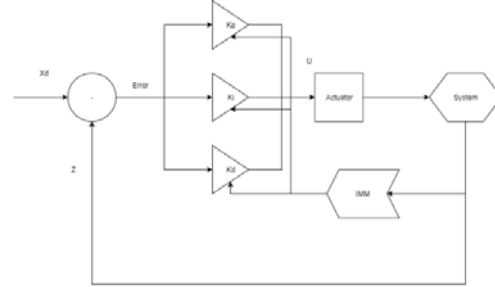


Fig. 3: IMM adaptive control strategy

II. SYSTEM MODEL

Two possible models can be used to describe the angular position and velocity of the elevation and inclination of the subsystem. Within the derivation of the rotational dynamic equations and the subsequent state space models, elevation is represented by (θ) and the telescope incline is represented by (ϕ) . The first model is completely linear and is used to assess the Linear Kalman Filters ability of estimating the states of a non linear system. The second model has varying dependent system parameters and is used to produce the true system behaviour and the state estimates using the Unscented Kalman filter. The two models are a variant on the rotational dynamic equations that are defined by the moment of inertia (I), the rotational damping coefficient (c), and the torsional spring constant (k).

A. Linear Model

The linear model of the subsystem assumes that all system parameters remain constant throughout the entire simulation. The entire subsystem is described by two independent (non-coupled) differential equations that are defined by the moment of inertias ($I_{th,ph}$), rotational damping coefficients ($c_{1,2}$), torsional spring constants ($k_{1,2}$), and input torques ($T_{1,2}(t)$) associated to each respective axis/DoF [8].

The following differential equations represent the building block of our system simulation. Equation 1 can be used to describe the states associated with the Elevation axis, while Equation 2 can be used to describe the states associated with the Inclination axis.

$$I_{th}\ddot{\theta} + c_1\dot{\theta} + k_1\theta = T_1(t) \quad (1)$$

$$I_{ph}\ddot{\phi} + c_2\dot{\phi} + k_2\phi = T_2(t) \quad (2)$$

An important concept is to know that the moment of inertias for both axes, although condensed into a single value, are

actually the sum of all moment of inertias of individual components rotating about a defined axis. The following equation shows the resulting moment of inertias.

$$I_{th,ph} = I_1 + I_2 + \dots + I_n$$

Given our particular system, the rotational spring constants are taken to be zero because the shafts are only used as pivot points and are not used to transmit power. This results in the additional simplification of the dynamics of our system to the following two equations.

$$I_{th}\ddot{\theta} + c_1\dot{\theta} = T_1(t) \quad (3)$$

$$I_{ph}\ddot{\phi} + c_2\dot{\phi} = T_2(t) \quad (4)$$

B. Non-Linear Model

The non linear model is described by the same differential equations used in the previous section, but the moment of inertia for the Elevation axis is directly dependent on the incline angle of the telescope. The linear model assumes that the telescope (represented by a hollow cylinder) maintains a constant orientation with respect to the reference coordinate system. This constant telescope position suggests that the telescope is constrained to only rotate about the X axis and therefore its movement is restricted to the YZ plane. For the non linear model, as the telescope incline angle changes from (0°) measured from the YZ plane, the moment of inertia for the telescope is no longer described by an axis of rotation about the principle X - axis. As a result, the rotation of the telescope is then defined by an arbitrary axis distributed within the relative XZ plane of the telescope.

C. State Space Representation

The following information describes the derivation of the state space representation of our subsystem. By placing our highest derivative term on the left hand side of the equation, and all lower derivative terms on the right, we obtain an expression for the angular accelerations of our subsystem.

$$\ddot{\theta} = -\frac{k_1}{I_{th}(\phi)}\theta - \frac{c_1}{I_{th}(\phi)}\dot{\theta} + \frac{1}{I_{th}(\phi)}T_1(t)$$

$$\ddot{\phi} = -\frac{k_2}{I_{ph}}\phi - \frac{c_2}{I_{ph}}\dot{\phi} + \frac{1}{I_{ph}}T_2(t)$$

Given this formulation, we can define our state variables as (θ) which represents the elevation angle, (ϕ) which represents the inclination angle, ($\omega_{th} = \dot{\theta}$) which represents the angular velocity in elevation, and ($\omega_{ph} = \dot{\phi}$) which represents the angular velocity in inclination [1].

$$x = \begin{bmatrix} \theta \\ \omega_{th} \\ \phi \\ \omega_{ph} \end{bmatrix}$$

By subbing in our state variables into the differential equations, we obtain the following result.

$$\dot{\theta} = \omega_{th}$$

$$\dot{\omega}_{th} = -\frac{k_1}{I_{th}(\phi)}\theta - \frac{c_1}{I_{th}(\phi)}\omega_{th} + \frac{1}{I_{th}(\phi)}T_1(t)$$

$$\dot{\phi} = \omega_{ph}$$

$$\dot{\omega}_{ph} = -\frac{k_2}{I_{ph}}\phi - \frac{c_2}{I_{ph}}\omega_{ph} + \frac{1}{I_{ph}}T_2(t)$$

Once the state variables are represented in the differential equations, we constructed our System Matrix (A), Input matrix (B), System Input (u), and Measurement matrix (C) and expressed our system dynamics in state space form [1].

$$\dot{x} = Ax + Bu$$

$$z = Cx$$

$$\dot{x} = \begin{bmatrix} 0 & 1 & 0 & 0 \\ -\frac{k_1}{I_{th}(\phi)} & -\frac{c_1}{I_{th}(\phi)} & 0 & 0 \\ 0 & 0 & 0 & 1 \\ 0 & 0 & -\frac{k_2}{I_{ph}} & -\frac{c_2}{I_{ph}} \end{bmatrix} \begin{bmatrix} \theta \\ \omega_{th} \\ \phi \\ \omega_{ph} \end{bmatrix} + \begin{bmatrix} 0 & 0 \\ \frac{1}{I_{th}(\phi)} & 0 \\ 0 & 0 \\ 0 & \frac{1}{I_{ph}} \end{bmatrix} \begin{bmatrix} T_1(t) \\ T_2(t) \end{bmatrix}$$

$$z = \begin{bmatrix} 1 & 0 & 0 & 0 \\ 0 & 1 & 0 & 0 \\ 0 & 0 & 1 & 0 \\ 0 & 0 & 0 & 1 \end{bmatrix} \begin{bmatrix} \theta \\ \omega_{th} \\ \phi \\ \omega_{ph} \end{bmatrix}$$

D. System Parameters

The following table shows the system parameters used during the simulation process. Once again, the shaft spring constants for the system are taken to be zero and the damping coefficient was assumed to be ($4Nm \cdot s/rad$). The design would ideally operate uninhibited by friction and therefore the damping coefficient was taken to be small. All moment of inertias were calculated using simple geometries of the primary components of the design, the densities of their anticipated materials, and their associated volumes.

TABLE I: System Parameters

DOF	$I (kg \cdot m^2)$	$c (Nm \cdot s/rad)$	$k (N/rad)$
Elevation	0.70-1.66	4	0
Azimuth	1.76	4	0

E. System and Measurement Noise Covariance:

To mimic the true operating characteristics of the system in the real world, noise was added at the system and measurement level. The added noise was Gaussian and possessed a mean value of (0). The variance of the added noise at the system and measurement level was defined by the System Noise and Measurement Noise covariances (Q , R) [3].

$$Q = \begin{bmatrix} 1 \times 10^{-5} & 0 & 0 & 0 \\ 0 & 1 \times 10^{-6} & 0 & 0 \\ 0 & 0 & 1 \times 10^{-5} & 0 \\ 0 & 0 & 0 & 1 \times 10^{-6} \end{bmatrix}$$

$$R = \begin{bmatrix} 6 \times 10^{-3} & 0 & 0 & 0 \\ 0 & 6 \times 10^{-5} & 0 & 0 \\ 0 & 0 & 6 \times 10^{-3} & 0 \\ 0 & 0 & 0 & 6 \times 10^{-5} \end{bmatrix}$$

A convenient understanding of the System Covariance is that it qualitatively describes whether your system is operating as theoretically intended. If your (Q) matrix contains high values, it implies that your system model is a poor description of the true states and that your true system behaviour is not well known. The Measurement Covariance matrix (R) represents the inaccuracies in your measurement devices. Overall, the filtering strategies that were applied to a system are attempting to estimate the true states of the system given its deviations from your system model (defined by Q), and the errors contained within your measurement system (defined by R).

To simulate the unanticipated system behaviour resulting from system noise (w) and the measurement noise (v), our discretized state space model is described by the following equations.

$$x_{k+1} = Ax_k + Bu_k + w_k$$

$$z_{k+1} = Cx_{k+1} + v_{k+1}$$

III. PID CONTROLS

Due to the 2DoF of the design, this system requires two independent PID controllers. The first controls the angular position of the Elevation axis, while the second controls the Inclination of the telescope. Once again, because the simulation operates in discrete time steps, the PID control equation is shown by Equation 5 where (k_p, k_i, k_d) represent the proportional, integral, and derivative gains, Int_{prev} is the sum of the area under the error curve for the previous time steps, and (E_k) represents the error between the pointing of the telescope and the location of the Moon [9].

$$u_{k+1} = k_p E_{k+1} + k_i \left[Int_{prev} + \left(\frac{E_{k+1} + E_k}{2} \right) T \right] + k_d \left(\frac{E_{k+1} - E_k}{T} \right) \quad (5)$$

To obtain an error between the pointing of the telescope and the position of the Moon, we required a desired trajectory of the Moon's movement as seen from the viewport of the ER-2 aircraft, and the desired Elevation and Inclination of the subsystem associated with the Moon location.

A. Desired Trajectory: Cylindrical Coordinates

To evaluate the system, a desired path resembling an infinity symbol was produced. We expected that the symbol would be appropriate because it offered simultaneous variation in the Elevation and Inclination control variables. The desired path was produced using cylindrical coordinates resulting from the following equations where ($t = 0^\circ - > 360^\circ$), (r) is the maximum distance of the Moon position with respect to the origin, and (z) is the vertical distance of the desired path from the origin.

$$\begin{aligned} x &= r \cos(t) \\ y &= r \cos(t) \sin(t) \\ z &= z \end{aligned}$$

The following plots show the resulting desired path when plotted in three dimensional space and as seen from above along the Z axis.

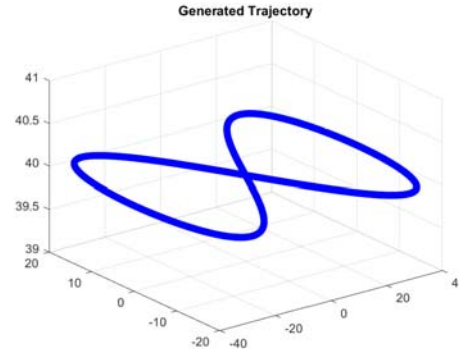


Fig. 4: Moon trajectory as seen from viewport of ER-2

IV. RESULTS:

The following plots found in Figure 5&6 show the Elevation and Inclination tracking abilities of the unfiltered non linear states in addition to the KF, UKF, and IMM state estimates all of which were using their own exclusive PID controllers. Additionally, the noisy measurements were also provided in Figure 7&8 to show the measurements that are used by the PID controller for the unfiltered scenario.

By reviewing the Elevation and Inclination states shown by Figure 5&6, all controllers whether it used the unfiltered measurements or the estimates from the KF, UKF, or IMM, appear to produce very similar results in accuracy and tracking.

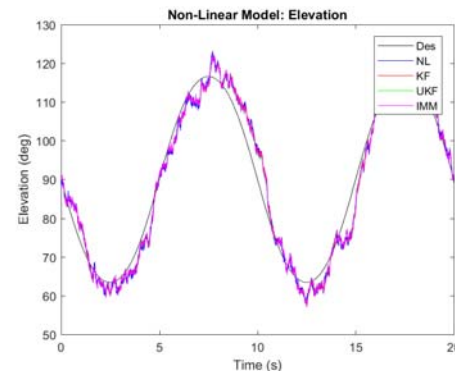


Fig. 5: Elevation

The extreme benefits of using estimated states as the input to your PID controller is shown by the reduction in torque produced by the actuators when comparing the system inputs for the Elevation/Inclination states of the unfiltered system

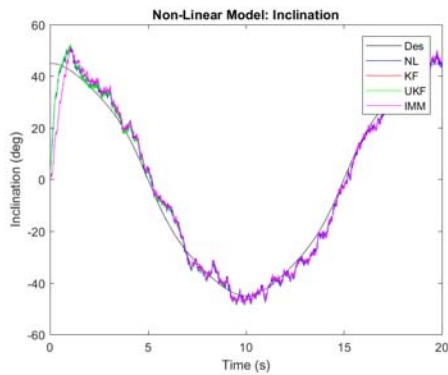


Fig. 6: Inclination

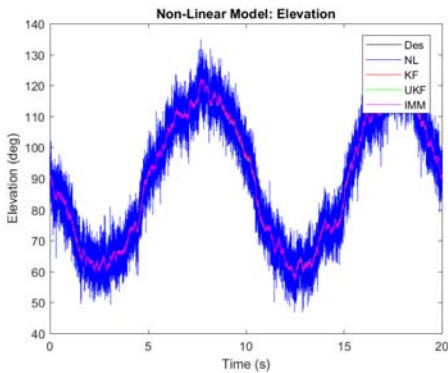


Fig. 7: Elevation with Measurement Noise

(NL), and the filtered systems (KL, UKF, IMM) shown by comparing Figure 9&10. You can only imagine the extreme duress and strain inflicted on the actuators when controlling the input based on the noisy error signals of an unfiltered system.

Although it was not obvious in Figure 5&6, the additional tracking accuracy when using the KF, UKF, and IMM state estimates to produce the PID error signal is shown by the Error Plot in Figure 11 and the RMSE values shown in Table II.

Upon inspection, we see that the RMSE values of all

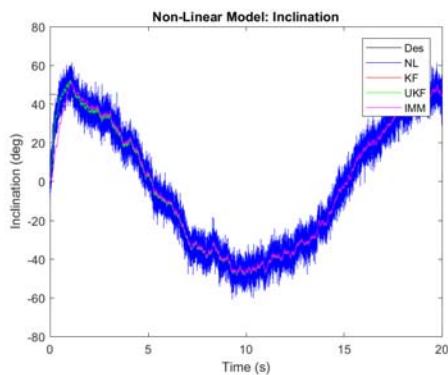


Fig. 8: Inclination with Measurement Noise

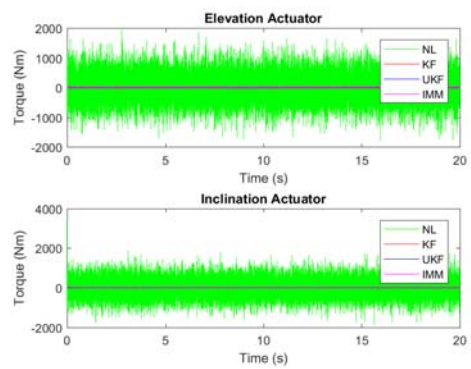


Fig. 9: System Input with noisy error signal

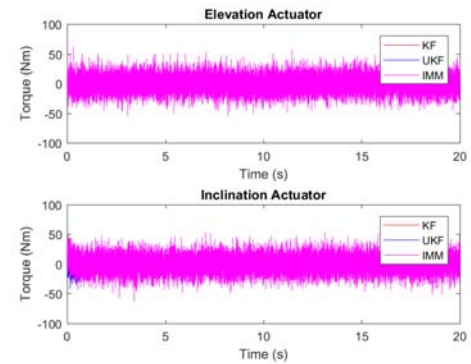


Fig. 10: System input with filtered error signals

three filtered simulations show approximately a (2.10°) improvement over the RMSE value produced by the unfiltered simulation. It is particularly important to emphasize that the RMSE values shown in Table II are produced using the PID error signal for each of the simulation scenarios, and are therefore a representation of the average error between the pointing of the telescope system and the location of the moon. Additionally, we can see that the results produced using the KF, and UKF are not significantly different. This suggests that although the system is non linear, its behaviour is not

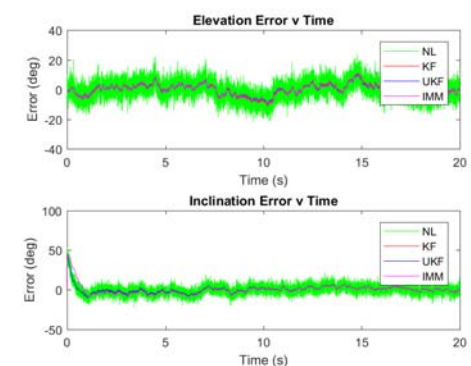


Fig. 11: Tracking error

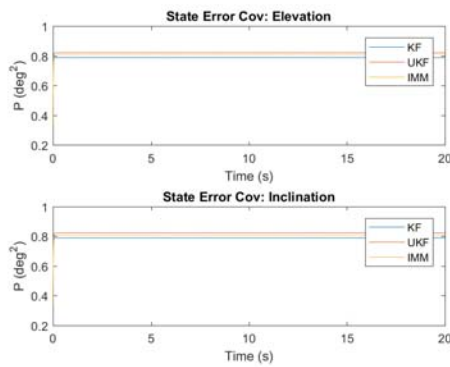


Fig. 12: State Error Covariance

significantly different than the linear system model used by the KF to produce the state estimates. This same conclusion can be drawn from the mode probabilities produced by the IMM simulation shown in Figure 13.

TABLE II: RMSE values for all simulations

DOF	Measurement	KF	UKF	IMM
Elevation (deg)	5.65	3.51	3.32	3.41
Inclination (deg)	7.01	5.39	5.40	6.95

The mode probabilities produced by the IMM filter prove that the system behaviour could be estimated to an equal degree of accuracy using the linear KF model or the Non Linear UKF model. This feature is shown by the consistent (50%) mode probability split shown in Figure 13. Given the Linear KF's ability to accurately estimate the system states and the similarities in State Error Covariance stability/convergence shown in Figure 12, it is highly recommended that only the KF estimates and filtering strategies be used for this particular system. Additionally, Figure 12 shows that all estimators show an extremely quick and stable convergence in State Error Covariance and achieve very similar steady state values. By using the simplest possible estimator the tracking system could benefit from the reduced KF computation time and improve the the tracking system speed in real time.

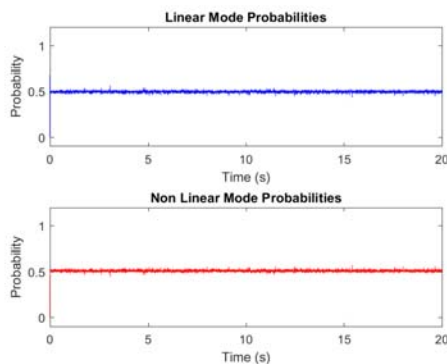


Fig. 13: IMM Mode Probabilities for 1) KF and 2) UKF

V. CONCLUSION

Based on the simulation results, we found that there were significant benefits of using filtered state estimates as the inputs to the PID controller when compared to using noisy system measurements. First, the reduced noise in the PID control inputs allow for a cleaner error signal when calculating the system input. Given less noise in the error signal, significantly less strain is placed on the actuators. The second benefit was an improved RMSE value when evaluating the error between the pointing angles of the subsystem and the position of the Moon. Even though the system model of the subsystem was (mildly) nonlinear, there appeared to be no significant advantage in terms of accuracy or stability when using the UKF or IMM compared to the more simple KF estimator. Given the equal ability of the KF and UKF to accurately estimate the system states, the adaptive IMM PID control strategy based on a linear and nonlinear model proved to be largely ineffective. The next phase of simulations will therefore use the IMM to distinguish between large and small Error modes of operation by interpreting the magnitude of error between the pointing of the subsystem and the position of the Moon. We expect that significant advantages in terms of accuracy could be produced by having a set of gains that control the system well during periods of large and small Error. This would allow for the IMM to toggle between two distinct modes of operation, the first being low error fine actuator control, and the second being high error large actuation control.

REFERENCES

- [1] S. A. Gadsden, ENGG 6090, Topic: "Linear Systems and Discrete Time Modeling", THRN 2313, School of Engineering, University of Guelph, Guelph, Ontario, Sept. 13, 2017.
- [2] S. A. Gadsden, ENGG 6090, Topic: "Observability, Controllability and Non Linear Systems", THRN 2313, School of Engineering, University of Guelph, Guelph, Ontario, Sept. 20, 2017.
- [3] S. A. Gadsden, ENGG 6090, Topic: "Kalman Filter and Extended Kalman Filter", THRN 2313, School of Engineering, University of Guelph, Guelph, Ontario, Oct. 4, 2017.
- [4] S. A. Gadsden, ENGG 6090, Topic: "Unscented Kalman Filter", THRN 2313, School of Engineering, University of Guelph, Guelph, Ontario, Oct. 25, 2017.
- [5] Pei H. Leong, Sanjeev Arulampalam, Thushara Abhayapala. "A Gaussian-Sum Based Cubature Kalman Filter for Bearings-Only Tracking", *IEEE Transactions on Aerospace and Electronic Systems*, Vol. 49 (2), pp. 1161-1177, Aug. 15 2012.
- [6] E. Mazor, A. Averbuch, Y. Bar-Shalom, J. Dayan, "Interacting Multiple Model Methods in Target Tracking: A Survey," *IEEE Transaction on Aerospace and Electronic Systems*, Vol. 34 (1), pp. 103-124, Jan. 1998.
- [7] Sungpil Yoon, John Lundberg, "Equations of Motion for a Two-Axes Gimbal system", *IEEE Transactions on Aerospace and Electronic Systems*, Vol. 37 (3), pp. 1083-1095, Jul. 2001.
- [8] W. Bolton, *Mechatronics: Electronic Systems in Mechanical and Electrical Engineering Ed. 5*. England: Pearson Education Limited, 2011, pp. 280-298.
- [9] W. Bolton, *Mechatronics: Electronic Systems in Mechanical and Electrical Engineering Ed. 5*. England: Pearson Education Limited, 2011, pp. 333-355.
- [10] S. A. Gadsden, "An Adaptive PID Controller Based on Bayesian Theory", *2017 ASME Dynamic Systems and Control Conference*, Tysons Corner, Virginia, 2017.
- [11] S. A. Gadsden, Y. Song, and S. R. Habibi, "Novel Model-Based Estimators for the Purposes of Fault Detection and Diagnosis", *IEEE/ASME Transactions on Mechatronics*, Vol. 18 (4), pp. 1237-1249, 2013.